



CHORUS

This is the accepted manuscript made available via CHORUS. The article has been published as:

Reduction of the neutron imaginary potential off the stability line and its possible impact on neutron capture rates

A. V. Voinov, K. Brandenburg, C. R. Brune, R. Giri, S. M. Grimes, T. Massey, Z. Meisel, S. N.

Paneru, A. L. Richard, G. Perdikakis, and A. Falduto

Phys. Rev. C **104**, 015805 — Published 22 July 2021

DOI: [10.1103/PhysRevC.104.015805](https://doi.org/10.1103/PhysRevC.104.015805)

Reduction of neutron imaginary potential off the stability line and its possible impact on neutron capture rates

A.V. Voinov,^{*} K. Brandenburg, C.R. Brune, R. Giri,[†] S.M. Grimes,
T. Massey, Z. Meisel, S.N. Paneru,[‡] and A.L. Richard[‡]
Department of Physics and Astronomy, Ohio University, Athens, OH 45701, USA

G. Perdikakis and A. Falduto[§]
Department of Physics, Central Michigan University, Mt. Pleasant, MI 48859, USA
(Dated: June 25, 2021)

The effect of the isovector imaginary optical potential has been studied experimentally using the particle evaporation technique for the $^{11}\text{B} + ^{48}\text{Ca}$ reaction with a 21.8 MeV ^{11}B beam. Spectra of neutron, proton and α -particles emitted from the neutron rich compound nucleus ^{59}Mn have been measured and analyzed with traditional optical model potentials with their original parameterizations as well as with adjusted isovector imaginary components. It is shown that the isovector component of the imaginary potential is indispensable in the reproduction of proton and α -particle yields from this reaction, and even needs to be enhanced compared to the suggestions of the original model parameterizations. This can lead to important consequences for astrophysical reaction rate calculations.

INTRODUCTION

The optical model (OM) of nuclear reactions [1] is widely used for reaction cross section calculations. The model suggests that a nucleus interacts with a particle through the mean field single particle potential consisting of real V and imaginary W components,

$$U = V + iW \quad (1)$$

where V is responsible for elastic scattering and W is for nuclear reactions. Solving the Schrodinger equation with such a potential allows for calculating transmission coefficients, T , which are responsible for probability of particle absorption by or emission from a nucleus thereby determining reaction cross sections.

OM potentials (OMP) are generally well established for stable nuclei [2]. For nuclei off the stability line, it is expected that the potentials are influenced by $(N-Z)/A$ values, where N, Z are the numbers of neutrons and protons in a nucleus, and $A = N + Z$. Bohr and Mottelson suggested [3] that the mean field single-particle potential would consist of the isoscalar U_0 and the isovector U_{iso} terms:

$$U = U_0 + U_{iso} = U_0 + \frac{1}{2}t_z \frac{(N-Z)}{A} U_{sym} \quad (2)$$

where $t_z = 1/2$ for protons and $t_z = -1/2$ for neutrons. U_{sym} is the symmetry potential which is related to the symmetry energy [4], which is an important quantity currently under investigation in both nuclear physics and astrophysics. It determines the structure of nuclei off the stability line as well as reaction rates in astrophysics, structure and composition of neutron stars [5].

Modern formulations of the OM take into account the isovector component in both the real and imaginary potentials. Here we use one of these formulations from

Ref. [6]. It is used in the Talys reaction code [7] and referred to as JLM semi-microscopic optical potential (it is referred to as JLMB in Ref. [6])) which is expressed as follows:

$$U(E) = \lambda_V(E)[V_0 \pm \lambda_{V_1}(E)\alpha V_1] + i\lambda_W(E)[W_0(E) \pm \lambda_{W_1}(E)\alpha W_1(E)] \quad (3)$$

where E is the energy of a neutron or proton, V_0, V_1, W_0, W_1 are real isoscalar, real isovector, imaginary isoscalar and imaginary isovector components, respectively, $\alpha = (N-Z)/A$, and $\lambda_V, \lambda_{V_1}, \lambda_W, \lambda_{W_1}$ are normalization factors for corresponding potential depths. Specific empirical formulas for normalization factors which are based on data for stable nuclei can be found in Refs. [6]. The W_1 component largely determines neutron/proton absorption and emission probabilities in nuclear reactions.

One of the important applications of the OM is the calculation of astrophysical reaction rates for medium mass and heavy nuclei. At astrophysical temperatures, reactions proceed mostly through the compound reaction mechanism. This is when the projectile a and the nucleus B fuse together forming a compound nucleus C which then decays by emitting ejectiles d_i such as gammas (γ), neutrons (n), protons (p) and alpha (α) particles, and produces the residual nuclei $D_i = C - d_i$. The theory of compound reactions which is known as the Hauser-Feshbach (HF) model in literature [8] suggests that the reaction cross section can be written as follows:

$$\frac{d\sigma_{d_i}(E_{d_i})}{dE_{d_i}} = \frac{\sigma_a^{fus} T_{d_i}(E_{d_i}) \rho_{D_i}(E_{D_i}^*)}{\sum_{j=1}^A \left[\int_{E_{d_j}} T_{d_j}(E_{d_j}) \rho_{D_j}(E_{D_j}^*) dE_{d_j} \right]}, \quad (4)$$

where $\sigma_a^{fus} = \pi \cdot T_a / k^2$, T_a and T_b are the transmission coefficients in the incoming and outgoing channels, respectively, k is the wave number, and ρ_{B_i} is the level density

of the residual nuclei D_i . A spin factor in σ_a^{fus} and the summation over spins and orbital momenta in Eq. (4) are omitted for simplicity of discussion. Transmission coefficients determine the probability of absorption and emission of particles and γ -rays. Particle coefficients are calculated from the optical model in Eqs. (1)-(3). Level density calculations are based on semi-empirical or microscopic models. The special interest of this study is to understand the role of the neutron OMP in calculating reaction rates for the rapid neutron capture (n, γ) reactions that are believed to be responsible for creation of about half of neutron-rich nuclei heavier than iron [9]. For neutron energies relevant to astrophysics (about hundreds keV), emission of protons from a neutron rich compound nucleus is generally energetically forbidden, and emission of α -particles is suppressed by the Coulomb barrier. For stable nuclei neutron transmission coefficients T_n are much larger than T_γ for γ -rays. Therefore, the denominator in Eq. 4 is overwhelmingly determined by the outgoing neutron coefficient $T_{d_j} = T_n$, which cancels out with the $T_a = T_{n_i}$ in an input channel $n+A$, so the cross section remains dependent only on T_{γ_j} and ρ_{D_j} in an outgoing channel. This is the reason of why uncertainties of neutron OMP are usually neglected in calculating (n, γ) reaction rates and the focus of studies has been on constraining γ -strength functions which determine T_γ , and level densities [10–12] to reduce uncertainties in calculations.

For nuclei off the stability line OMP are highly uncertain because they are not constrained by experimental data. Moreover, the paper of Ref. [13] indicates that the normalization factor λ_{W_1} in Eq. (3) might be underestimated for neutron rich nuclei. It requires a large enhancement to be able to reproduce the strength function of neutron resonances for some nuclei. Enhancement of λ_{W_1} leads to reduction of the total imaginary potential in Eq. (3) which, in turn, results in reduction of neutron transmission coefficients T_n to the point at which T_n and T_γ become comparable. In this case (n, γ) cross section will be influenced by T_n according to Eq. (4). If this scenario is correct for all neutron-rich nuclei, the current estimation of reaction rates for neutron capture nucleosynthesis via r-process [13] and may be via i-process as well, need to be substantially revised.

This paper suggests an experimental method to study the isovector component of the neutron OMP by measuring the yield of outgoing neutrons, protons and α -particles from the decay of the compound neutron-rich nucleus ^{59}Mn formed in the $^{11}\text{B} + ^{48}\text{Ca}$ reaction. The ratio of yields between different outgoing channels, according to HF theory, is sensitive to neutron transmission coefficients. If neutron transmission coefficients are smaller due to the diminishing value of the imaginary potential as suggested in Ref. [13], we expect to see an increase of proton and α -particle yields compared to the neutron one.

EXPERIMENT

The experiment was performed at the tandem accelerator of the Edwards Accelerator Laboratory using a 22 MeV ^{11}B beam. The 2 mg/cm² thick target was a pure calcium self-supported foil enriched to 96.2% with ^{48}Ca . The remaining 3.8% consisted of ^{40}Ca . The target was produced by the National Isotope Development Center, Oak Ridge, TN. A charged particle spectrometer was used to detect protons and α -particles. The spectrometer included five silicon detectors, two of which were located at 2 m from the target at 37.5 and 67.5 degrees, and the remaining three were at 127.5, 142.5 and 157.5 degrees at 1 m from the target. Detectors were mounted at the ends of the vacuum arms attached to the target chamber [14]. Additionally, the $\Delta E - E$ telescope consisting of 0.25 and 5 mm thick silicon detectors was mounted at an angle of 142 degrees and 20 cm from the target to measure high energy protons. The liquid scintillator NE213 neutron detector was setup at 137 cm from the target position, at an angle of 120 degrees. The beam was run in a pulsing and bunching mode with about 5 ns timing width. This allowed for measuring the time of flight (TOF) for charged particles and neutrons. Both the TOF and the energy deposited in the silicon detectors allowed for identifying charged particles and measuring their energy. For the energy calibration a thin carbon foil was used as a target. The known structure in the α -spectrum from the $^{11}\text{B} + ^{12}\text{C}$ reaction was used for the detector energy calibration. Neutron energies were determined by the TOF technique. The position of the γ -peak in the TOF spectrum was used as a calibration point for the absolute time calibration. The detector efficiency was determined from a separate experiment with the $^{\text{nat}}\text{Al}(d, n)$ reaction using a thick aluminum target which stops the beam. This reaction produces a calibrated neutron flux [15] which was used for the neutron detector efficiency calibration.

Extra precautions have been made to minimize target exposure to the air. The calcium foil was shipped in a vacuum container, and has been exposed to the air for less than 5 minutes while it was mounted on the target ladder and placed in the vacuum target chamber. Also, additional measurements have been performed to study possible contamination of the target material with oxygen and carbon. The latter is usually built up on the target during the beam run because of oil vapor which is present in the vacuum system due to the operation of oil-based vacuum pumps. Extra measurements have been performed on the ^{48}Ca target with smaller beam energies including 20, 18, and 16 MeV. Since the Coulomb barrier is 19.6 MeV, it is expected that the fusion cross section for the calcium nucleus decreases rapidly with decreasing beam energy from its original value of 22 MeV. For oxygen and carbon, the Coulomb barriers are 7.6 and 9.7 MeV, respectively, so that the cross sections should

not change much. These expectations have also been confirmed with theoretical calculations. Additionally, carbon and tungsten oxide foils were used as targets to measure charged particle yields. Comparing cross sections for different beam energies impinging on calcium, carbon and tungsten oxide targets allowed us to conclude that for the 22 MeV beam energy the possible light mass contribution to the spectra constitutes less than 10 percent and concentrated at low energies in the lab system, at around $\lesssim 4$ MeV.

There are statistical and systematic uncertainties for the particle yields. The statistical uncertainties account for less than about 2% for protons and α -particles and 0.1% for neutrons for energy integrated yields. Systematic uncertainties are related to the beam current integration (about 3%), neutron detector efficiency (about 6%), solid angles for charged particle detectors (about 10%). This sums up to about 7% for the total systematic uncertainty for the absolute neutron yield and about 10% for the yield of protons and α -particles. For the relative yield of protons to neutrons and α -particles to neutrons the uncertainty is estimated to be 12%.

MODEL CALCULATIONS

The proton, neutron and α -particle spectra from $^{11}\text{B} + ^{48}\text{Ca}$ reaction were first calculated with the Empire code [16] using the HF model of nuclear reactions [8]. Empire can use heavy ions in input channel and variety of level density and optical model parameterizations except the JLM model. The Empire code suggests two models to calculate the compound nucleus formation cross section. These are the simplified coupled-channel treatment of the heavy ion fusion and the distributed fusion barrier model. There is a lack of experimental data for the fusion cross sections of ^{11}B -induced reactions in this energy range, however, our previous study of $^7\text{Li} + ^{68,70}\text{Zn}$ reactions showed that the coupled channel approach agrees well with experiment [17]. For the 21.8 MeV ^{11}B beam the barrier distribution model results in 380 mb for the fusion cross section versus 420 mb for the coupled channel one. We started with the coupled channel approach and final adjustments were made based on comparison with experimental data

For transmission coefficients, Empire uses the A.J. Koning and J.P. Delaroche (KD) potentials [18] as a default option for neutrons and protons and the potential by V. Avrigeanu et al [19] for α -particles. For level densities, following models were tested: the back shifted Fermi-gas (BSFG) model and the model based on the Gilbert and Cameron (GC) approach [20] - both with parameter systematics from the Research Input Parameter Library (RIPL) [2], the BSFG model with parameters from von Egidy et al [21], and the model based on the microscopic calculations (MC) of Ref. [22].

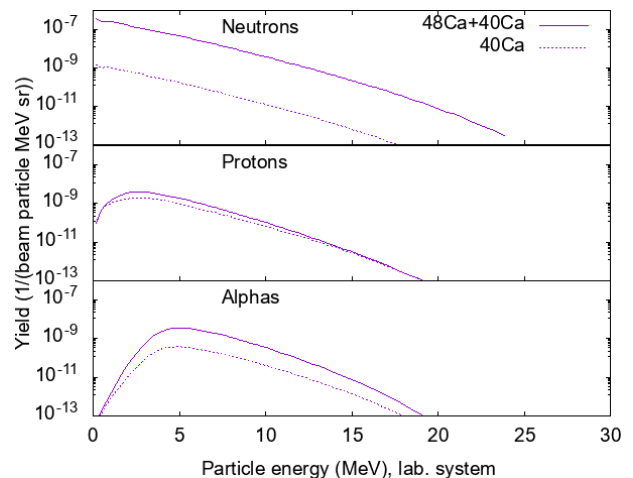


FIG. 1. Empire calculations showing fraction of expected contribution of ^{40}Ca target contamination. Full line are spectra from the target containing 96.2% of ^{48}Ca and 3.8% of ^{40}Ca . Dotted lines show contribution from 3.8% ^{40}Ca contaminant. Calculations were performed with BSFG Egidy level density parameterization.

The 21.8 MeV ^{11}B beam loses about 6 MeV in the 2 mg/cm^2 ^{48}Ca target. According to the Empire coupled channel calculations, the fusion cross section drops from 420 mb when the beam enters the target to 2 mb when beam exits the target. Therefore the experimental spectra were considered to be the sum of the spectra produced at different beam energies with different fusion cross sections while the beam travels through the target. In order to compare model calculations with experiment, the sum spectra were modeled taking into account the beam energy and fusion cross section changes. Therefore in calculations, the target was subdivided into 20 slices, the particle spectra were calculated for each of them, and then spectra were converted to the laboratory frame and summed up to produce final model spectra which can be compared with experimental ones. Energy losses in the target for outgoing protons and α -particles have also been taken into account. Because of the rapid decrease of the cross section while the beam passes through the target, the final spectra were calculated in units of particle yield from the target instead of units of cross section.

The ^{48}Ca target contained 3.8% of ^{40}Ca contaminant, therefore, calculations were run for both of these target nuclei and resulting spectra were then summed up weighted with corresponding fractions. According to calculations presented in Fig. 1, the resulting cross sections for the neutron and α channels are overwhelmingly dominated by reactions on ^{48}Ca , however, cross sections for the proton channel contain about 50% contribution from ^{40}Ca at low energies and close to 100% at higher proton energies.

RESULTS AND DISCUSSION

For the analysis, we used experimental spectra measured at backward angles since they are expected to contain minimal contributions (if any) from non-compound reaction mechanisms such as direct and/or pre-equilibrium ones. Therefore, experimental alpha and proton spectra taken at 142 degrees and the neutron spectrum measured at 120 degrees are presented in Fig.2 (top panel) along with compound model calculations using different input level density models. Experimental proton and α -particle spectra are shown in the energy range above the Coulomb barrier of emitted particles (greater than around 2 and 5 MeV in the lab system respectively), since optical model calculations are more robust for energies above the Coulomb barrier and contribution from light target contaminants is believed to be negligible at higher energy ranges. High energy limits are determined by counting statistics only. Low and high energy limits for the neutron spectrum are determined by the detector threshold and the high energy limit of NE213 neutron detector efficiency measurements. Light elements target contaminants are less important here since neutron yield from the ^{48}Ca target is about two orders of magnitude higher than the yields of protons and α particles.

According to the calculations the main decay channel of the compound ^{59}Mn nucleus is expected to be the neutron one. It constitutes 400 mb out of the 420 mb of the fusion cross section for the 21.8 MeV ^{11}B beam. The rest is shared between protons and α -particles. In the neutron energy range of up to 10 MeV measured in the experiment, along with first chance neutrons ($^{11}\text{B}, n$), an almost equal contribution comes from ($^{11}\text{B}, 2n$) and ($^{11}\text{B}, 3n$) channels. For the proton and α channels, about 60% comes from the first chance decay ($^{11}\text{B}, (\alpha/p)$), 35% from ($^{11}\text{B}, n(\alpha/p)$) and 5% from ($^{11}\text{B}, 2n(\alpha/p)$). Reaction Q-values are 12.20, 9.15, and 11.16 MeV for the first chance emission of neutrons, protons, and α -particles respectively.

Comparison of Empire calculations with experiment shows that the absolute neutron yield is reproduced within experimental uncertainties (see Fig. 2). However, calculations underestimate proton and α -particle yields by a factor of about 2. Different level density inputs result in comparably small calculation spread at low energies which increases at higher energies. From a comparison of the shapes of spectra, one can see that the level density models based on the BSFG Egidy [21] approach follow the slope of experimental points better compared to other models. All models underestimate the absolute yield of α -particles in the whole energy range. For the protons, it appears that BSFG models reproduce the high energy fraction well, but they underestimate the low energy fraction of the proton spectrum.

To study effect of the isovector imaginary potential on

TABLE I. Average ratios R between experimental and calculated spectra as defined by Eq. 5, and calculated $^{58}\text{Mn}(n, \gamma)$ capture rates for the temperature $T=10^9\text{K}$. Total uncertainties are shown in parentheses.

Model	R_n	R_p	R_α	$\frac{R_p}{R_n}$	$\frac{R_\alpha}{R_n}$	(n, γ) rates $\frac{\text{cm}^3}{\text{s.mol}}$
	$[E_1, E_2], \text{MeV}$					
	[2,10]	[8,18]	[6.5,14]			
KD	0.96(7)	0.60(7)	0.48(6)	0.63(10)	0.50(9)	2.32
KD _{adj} ¹	0.79(6)	0.73(9)	0.80(10)	0.92(11)	1.01(12)	1.64
KD _{adj} ²	0.98(7)	0.88(11)	1.00(12)	0.90(13)	0.92(14)	1.64
JLM	1.07(7)	0.68(8)	0.58(7)	0.64(11)	0.54(10)	2.08
JLMG	1.01(7)	0.69(8)	0.61(7)	0.68(11)	0.60(10)	1.98
JLM _{adj}	1.13(8)	0.77(9)	0.89(11)	0.68(12)	0.79(14)	1.67

particle evaporation spectra, we used the HF computer code developed at Ohio University [23]. This code allows one to input transmission coefficients for both incoming and outgoing particles and to parameterize level density models with the Fermi-gas approximation [24]. It also has a unique capability to calculate an angular distribution for outgoing particles so that particle spectra measured at a certain angle can be calculated more accurately. The angular distribution from compound reactions is symmetric about 90° in the center of mass frame [25] while both Empire and Talys codes assume it to be isotropic. The Talys computer code allows using both Koning and Delaroche and JLM OMPs but it does not allow heavy ions for the input reaction channel. Empire has the capability of using heavy ions in an input channel but does not allow JLM optical potential. Therefore, we imported transmission coefficients for the incoming ^{11}B ions calculated with the Empire code and transmission coefficients for neutron and protons calculated with JLM and Koning and Delaroche models from Talys into the Ohio HF code. Talys capabilities to adjust parameters of optical models were utilized for these calculations. The purpose of these calculations is to show that reduction of the total imaginary potential, which is assumed to be caused by enhancing the isovector imaginary potential, would improve the description of the experimental data. We did not attempt to come up with specific OM parameters and quantify their uncertainties because data obtained from our experiment are not sufficient to constrain all parameters of the optical model.

Imaginary potential adjustments were tested for both KD and JLM models. In Talys, the imaginary potential for the KD model can be scaled separately for neutrons and protons. Such a modification does not change the energy dependence of the potential. For the JLM model of Eq. 3, scalable parameters are λ_{W1} and λ_W , however, the factor λ_W affects neutron and proton potentials in the same direction that is not in accord with the conception of Eq. 1. Therefore, adjustment of only λ_{W1} parameter

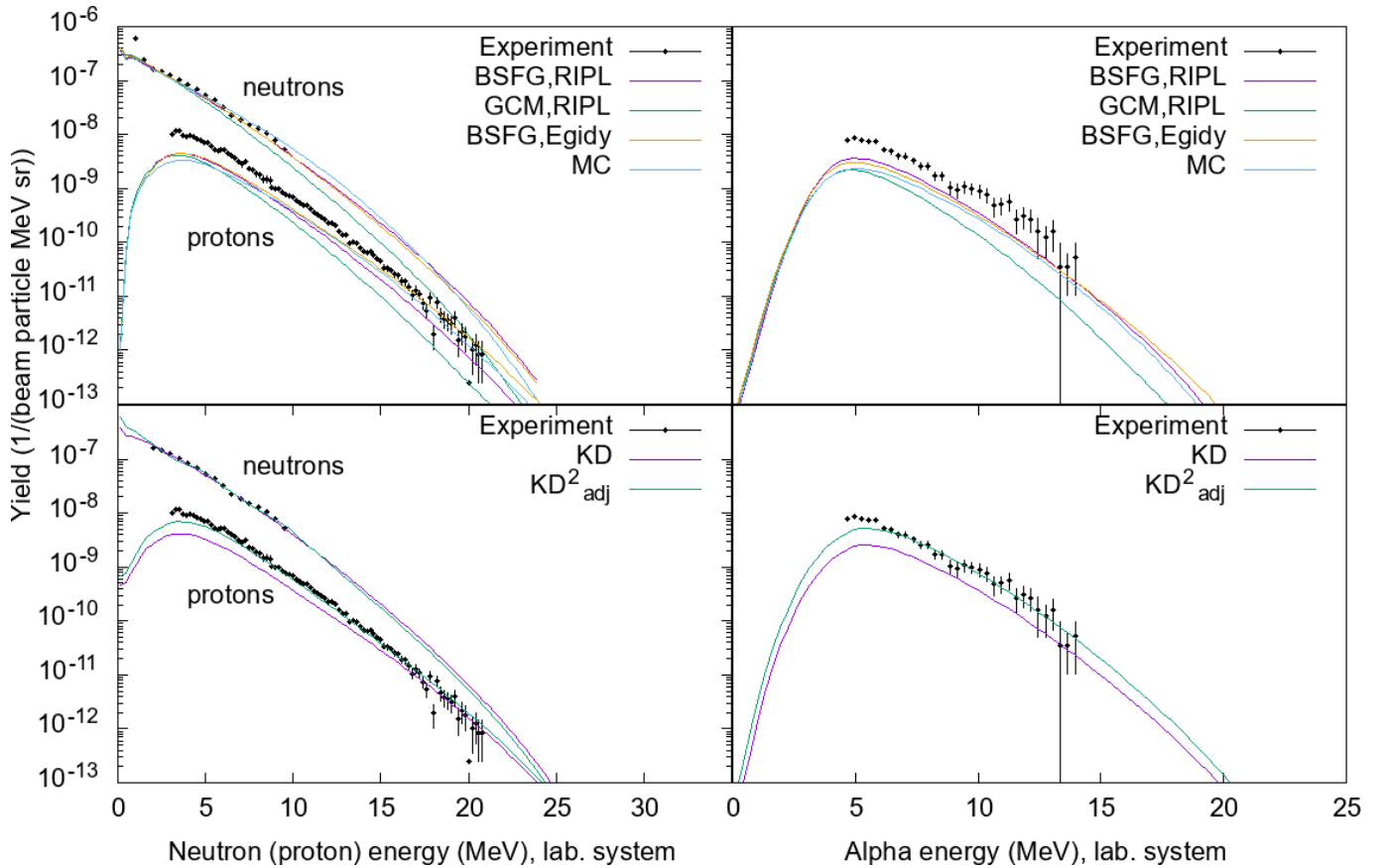


FIG. 2. Experimental and calculated spectra from the $^{11}\text{B} + ^{48}\text{Ca}$ reaction with 22 MeV boron beam. Experimental spectra are from 142 degrees (protons and α -particles, respectively) and from 120 degrees (neutrons). Calculations were performed with the Empire computer code [16] (top panel) with different input level density models and default fusion and optical model parameters discussed in the text. Bottom panel: calculations were performed with HF computer code [23] using the level density model from Ref. [21]. Calculations are shown with the original OMP from Ref.[18] (KD) and with the adjusted one (KD_{adj}^2) as described in the text.

was tested in calculations. This, however, unlike for the KD model, results in a change of the energy dependence of the total imaginary potential since all components including isoscalar W_0 , isovector W_1 and the scaling factor λ_{W_1} have different energy dependence.

Calculations were performed with the Ohio University HF code using the BSFG model by Egidy et al. [21] and the following OMP parameterizations:

- KD: Original parameterization of Koning and Delaroche model [18].
- KD_{adj}^1 : The total imaginary potential of the Koning and Delaroche model was empirically adjusted to the point when proton/neutron and α /neutron experimental yield ratios are reproduced with calculations within experimental uncertainties. The total original imaginary potential $W = \sum_i W_i$, $i=\text{V,D,SO}$, consisting of volume(V), surface(D), and spin-orbit(SO) terms was modified with the empirical adjustment factor k such that $W_i^{\text{mod}} =$

$W_i(1 \pm k)$, where "-" was used for neutrons and "+" for protons. k was empirically adjusted to the value of 0.8.

- KD_{adj}^2 : The same as KD_{adj}^1 but with the fusion cross section increased by a factor of 1.25 to reproduce absolute yields of neutron, proton and α -particles within uncertainties.
- JLM: Original parameterization of the JLM model [6].
- JLMG: the isovector imaginary normalization factor λ_{W_1} in Eq. eq:3 according to the prescription of Ref. [13].
- JLM_{adj} : The parameter λ_{W_1} in Eq. 3 was assumed to be an energy independent and empirically adjusted to the value of $\lambda_{W_1} = 4$ bringing the ratio of proton/neutron and α /neutron yields closer to experimental values. It resulted in a change of the

neutron and proton imaginary potential depths by factors of 0.5 and 1.5 respectively.

Values for adjustment factors for both KD and JLM models were empirically estimated with few iterations to reduce neutron transmission coefficients by factor of about two for the average emitted neutron energy of ≈ 3 MeV. The accuracy of these values were not studied at this point.

For the comparison between experiment and calculations the average ratio over data points was used in the following form:

$$R = \frac{1}{N} \sum_{i=1}^N \frac{Y_i^{cal}}{Y_i^{exp}}, \quad (5)$$

where $N \in [E_1, E_2]$ is the number of experimental points with energies between E_1 and E_2 .

The energy interval $[E_1, E_2]$ was chosen such that shape of calculated spectra in this energy range would be in a good visible agreement with experimental ones. This was done by evaluating the function $R(E_i) = Y^{cal}(E_i)/Y^{exp}(E_i)$, where $i=1..N$ and $N \in [E_1, E_2]$. The function was found to be slowly varying in the interval $[E_1, E_2]$ indicating the consistency between experimental and calculated spectra shapes but it sharply drops at $E_i < E_1$ due to a decrease of the calculated yield compared to experimental one that can be seen from Fig. 2. This might indicate that the low-energy region is more vulnerable to other uncertainties in calculations which might include uncertainties in level densities at higher excitation energies (> 20 MeV), uncertainties related to contributions from 2nd, and 3^d chances of particle emissions which are more difficult to model because more model parameters are involved. Possible contributions from light target contaminants, as was discussed earlier, might also explain this discrepancy.

Values of R are presented in Table and spectra calculated with the original KD and the adjusted KD_{adj}^2 models are shown in the low panel of Fig. 2. One can see that the KD used in the Ohio HF code gives similar results to Empire indicating consistency between codes. R values indicate that calculations reproduce the neutron spectrum well but they underestimate proton and α -absolute yields by factor of about 2. The KD_{adj}^1 model adjustment allowed satisfactory (within experimental uncertainties) description of proton/neutron and α /neutron yield ratios but underestimates absolute values by the same factor of ≈ 0.8 . This might indicate that the fusion cross section is underestimated by calculations. Calculations with the adjusted fusion cross section by a factor of 1.25 (KD_{adj}^2) brought calculated absolute yields to an agreement with experimental data.

Adjustments of the JLM model result in similar tendency as for the KD model, in the sense that increasing the isovector imaginary potential leads to an increase of

calculated proton and α yields, bringing R_p and R_α closer to one. However, contrary to KD, it also results in an increase of R_n , keeping proton/neutron and α /neutron yield ratios underestimated by calculations (both R_p/R_n and R_α/R_n remain less than one by about 20%) making it impossible to reach agreement with absolute yields for all particles simultaneously. The reason for this is that reduction of the total neutron imaginary potential in the JLM model affects low-energy neutron transmission coefficients to a greater extent compared to the KD model. Because of competition between low and high energy neutrons, decreasing low-energy transmission coefficients causes cross section for higher energy neutrons to increase. Effect of the imaginary potential reduction on the spectra of the first chance neutrons emitted from the compound nucleus ^{59}Mn is shown in Fig. 3. For the KD model it results in an increase of the low-energy neutrons ($\lesssim 2$ MeV) and in a decrease of the higher energy ones, while for the JLM model it has an opposite effect.

Despite other potential uncertainties in calculations, which prevent us from making a definite conclusion, results obtained in this work indicate that the role of the isovector optical potential might be more important for neutron rich nuclei than assumed by existing OM parameterizations. Therefore, the isovector potential may have a larger impact on astrophysical reaction rates of neutron captures off stability.

The compound nucleus ^{59}Mn is within the i-process nucleosynthesis path, therefore, it is interesting to see how the suggested renormalizations of the isovector imaginary potential can potentially affect reaction rates. We performed Talys calculations with default γ -strength and level density models for the Maxwellian-averaged $^{58}\text{Mn}(n, \gamma)$ rates at the temperature of $T=10^9\text{K}$ relevant to r-process nucleosynthesis. The neutron capture by ^{58}Mn is an inverse process to the neutron decay of the ^{59}Mn compound nucleus so that the same optical model parameters can be used for calculations. The indicated temperature corresponds to the average neutron energy of about 100 keV. Results of calculations presented in Table show that an increase of the isovector component of the imaginary potential from KD to $KD_{adj}^{1(2)}$ and from JLM to JLM_{adj} parameterizations results in decrease of the neutron capture rates by 30% and 20% respectively, while renormalization suggested in Ref. [13] (JLMG) reduces it by 4% only. However, these numbers are expected to be sensitive to the γ -strength function and level density model parameterizations for the compound nucleus ^{59}Mn .

An analysis of experimental particle evaporation spectra performed in this work indicates needs for the reduced total imaginary potential, which is supposedly caused by enhancing its isovector component, compared to parameterizations in Refs. [6, 13, 18]. This conclusion is in qualitative accord with the results of Ref. [13] but suggests a more dramatic role of the imaginary isovector poten-

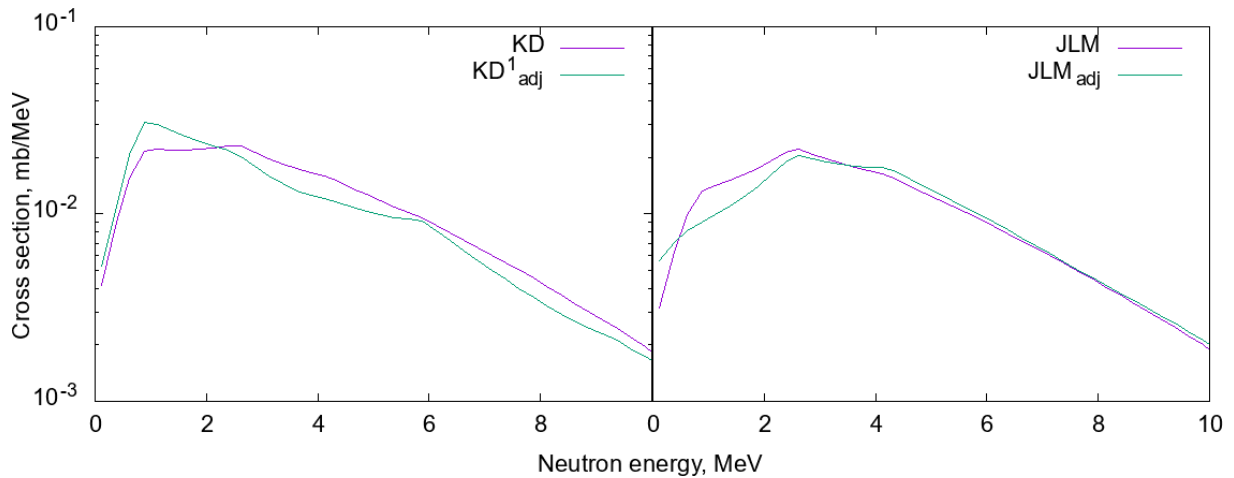


FIG. 3. Spectra of first chance neutrons calculated with original and adjusted parameterizations for KD (left panel) and JLM (right panel) models. Fluctuations are caused by competitions between neutrons with different orbital momenta.

tial. The enhanced isovector optical potential could have a substantial impact on calculations of cross sections and reaction rates for neutron rich nuclei in astrophysical processes.

We note however, that even though reduction of the neutron imaginary potential helped to reproduce experimental particle spectra from the $^{11}\text{B} + ^{48}\text{Ca}$ reaction, other optical potential parameters remain unconstrained and might potentially affect calculations. Therefore, obtained results require further experimental confirmations, specifically, for low-neutron energies down to astrophysical important ones (around 100 keV). Normally, optical potentials should be able to reproduce elastic scattering and reaction cross sections. However, since there are experimental limitations for studying neutron induced reactions away from stability line, the experimental methods based on studying decay channels of compound nuclei might be an useful tool to infer the isovector component of the OMP for nuclei off the stability line with current and prospective radioactive beam facilities.

ACKNOWLEDGMENTS

This work was supported in part by the U.S. Department of Energy under Grants No. DE-FG02-88ER40387, No. DE-NA0003883, No. DE-NA0003909, and No. DE-SC0019042. We benefited from support by the National Science Foundation under Grant No. PHY-1430152 (JINA Center for the Evolution of the Elements). G.P. and A.F. acknowledge support from the College of Science and Engineering of Central Michigan University for the procurement of the ^{48}Ca target. A.V. acknowledges discussions with S. Goriely during the preparation of this manuscript.

* voinov@ohio.edu

† Present address: Holmes Community College, Ridgeland, MS 39157, USA

‡ Present address: National Superconducting Cyclotron Laboratory, Michigan State University, East Lansing, MI 48824, USA

§ Present address: Institut für Kernphysik, Technische Universität Darmstadt, D-64289 Darmstadt, Germany

- [1] H. Feshbach, The optical model and its justification, *Annual Review of Nuclear Science* **8**, 49 (1958), <https://doi.org/10.1146/annurev.ns.08.120158.000405>.
- [2] R. Capote, M. Herman, P. Obložinský, P. G. Young, S. Goriely, T. Belgya, A. V. Ignatyuk, A. J. Koning, S. Hilaire, V. A. Plujko, M. Avrigeanu, O. Bersillon, M. B. Chadwick, T. Fukahori, Z. Ge, Y. Han, S. Kailas, J. Kopecky, V. M. Maslov, G. Reffo, M. Sin, E. S. Soukhovitskii, and P. Talou, Reference input parameter library (ripl-3), *Nucl. Data Sheets* **110**, 3107 (2009), <https://www-nds.iaea.org/RIPL-3>.
- [3] A. Bohr and B. R. Mottelson, *Nuclear Structure* (W. A. Benjamin, New York, 1969).
- [4] C. Xu, B.-A. Li, and L.-W. Chen, Symmetry energy, its density slope, and neutron-proton effective mass splitting at normal density extracted from global nucleon optical potentials, *Phys. Rev. C* **82**, 054607 (2010).
- [5] M. Baldo and G. Burgio, The nuclear symmetry energy, *Progress in Particle and Nuclear Physics* **91**, 203 (2016).
- [6] E. Bauge, J.-P. Delaroche, and M. Girod, *Phys. Rev. C* **63**, 024607 (2001).
- [7] A. J. Koning, S. Hilaire, and M. C. Duijvestijn, Talys-1.2, in *Proceedings of the International Conference on Nuclear Data for Science and Technology (April 22-27, 2007, Nice, France)*, edited by O. Bersillon, F. Gunsing, E. Bauge, R. Jacqmin, and S. Leray (EDP Sciences, 2008) p. 211.
- [8] W. Hauser and H. Feshbach, The inelastic scattering of neutrons, *Phys. Rev.* **87**, 366 (1952).
- [9] T. Kajino, W. Aoki, A. Balantekin, R. Diehl, M. Famiano, and G. Mathews, Current status of r-process nucle-

- osynthesis, *Progress in Particle and Nuclear Physics* **107**, 109 (2019).
- [10] A. C. Larsen, A. Burger, S. Goriely, M. Guttormsen, A. Gorgen, T. K. Eriksen, T. W. Hagen, S. Harissopoulos, H. T. Nyhus, T. Renstrom, S. Rose, I. E. Ruud, A. Schiller, S. Siem, G. M. Tveten, and A. Voinov, *Acta Phys. Pol.* **B44**, 563 (2013).
- [11] S. N. Liddick, A. Spyrou, B. P. Crider, F. Naqvi, A. C. Larsen, M. Guttormsen, M. Mumpower, R. Surman, G. Perdikakis, D. L. Bleuel, A. Couture, L. Crespo Campo, A. C. Dombos, R. Lewis, S. Mosby, S. Nikas, C. J. Prokop, T. Renstrom, B. Rubio, S. Siem, and S. J. Quinn, Experimental neutron capture rate constraint far from stability, *Phys. Rev. Lett.* **116**, 242502 (2016).
- [12] S. Nikas, G. Perdikakis, M. Beard, R. Surman, M. R. Mumpower, and P. Tsintari, Propagation of hauser-feshbach uncertainty estimates to r-process nucleosynthesis: Benchmark of statistical property models for neutron rich nuclei far from stability (2020), arXiv:2010.01698 [nucl-th].
- [13] S. Goriely and J.-P. Delaroche, The isovector imaginary neutron potential: A key ingredient for the r-process nucleosynthesis, *Physics Letters B* **653**, 178 (2007).
- [14] A. V. Voinov, S. M. Grimes, C. R. Brune, M. J. Hornish, T. N. Massey, and A. Salas, Test of nuclear level density inputs for Hauser-Feshbach model calculations, *Phys. Rev. C* **76**, 044602 (2007).
- [15] T. N. Massey, S. Al-Quraishi, C. E. Brient, J. F. Guillemette, S. M. Grimes, D. Jacobs, J. E. O'Donnell, J. Oldendick, and R. Wheeler, A measurement of the $^{27}\text{Al}(d,n)$ spectrum for use in neutron detector calibration, *Nucl. Sci. Eng.* **129**, 175 (1998).
- [16] M. Herman, R. Capote, B. Carlson, P. Obložinský, M. Sin, A. Trkov, H. Wienke, and V. Zerkin, Empire: Nuclear reaction model code system for data evaluation, *Nucl. Data Sheets* **108**, 2655 (2007).
- [17] A. V. Voinov, T. Renstrøm, D. L. Bleuel, S. M. Grimes, M. Guttormsen, A. C. Larsen, S. N. Liddick, G. Perdikakis, A. Spyrou, S. Akhtar, N. Alanazi, K. Brandenburg, C. R. Brune, T. W. Danley, S. Dhakal, P. Gastis, R. Giri, T. N. Massey, Z. Meisel, S. Nikas, S. N. Paneru, C. E. Parker, and A. L. Richard, Level densities of $^{74,76}\text{Ge}$ from compound nuclear reactions, *Phys. Rev. C* **99**, 054609 (2019).
- [18] A. J. Koning and J. P. Delaroche, Local and global nucleon optical models from 1 keV to 200 MeV, *Nucl. Phys.* **A713**, 231 (2003).
- [19] V. Avrigeanu, P. E. Hodgson, and M. Avrigeanu, *Phys. Rev. C* **49**, 2136 (1994).
- [20] A. Gilbert, F. S. Chen, and A. G. W. Cameron, *Can. J. Phys* **43**, 1248 (1965).
- [21] T. von Egidy and D. Bucurescu, *Phys. Rev. C* **80**, 054310 (2009).
- [22] S. Goriely, S. Hilaire, and A. J. Koning, *Phys. Rev. C* **78**, 064307 (2008).
- [23] S. M. Grimes, A user's manual for the Hauser-Feshbach code HF2002, Internal report INPP 04-03 (2004).
- [24] H. A. Bethe, An attempt to calculate the number of energy levels of a heavy nucleus, *Phys. Rev.* **50**, 332 (1936).
- [25] T. Ericson and V. Strutinski, Angular distribution in compound nucleus processes, *Nucl. Phys.* **8**, 284 (1958).